Real-Time Intraoperative Detection of Breast Cancer Axillary Lymph Node Metastases Using a Green Fluorescent Protein-Expressing Herpes Virus

David P. Eisenberg, MD, Prasad S. Adusumilli, MD,* Karen J. Hendershott, MD,* Sun Chung, MD,† Zhenkun Yu, MD, PhD,* Mei-Ki Chan, BS,* Michael Hezel, BS,* Richard J. Wong, MD,* and Yuman Fong, MD**

Objective: To investigate the use of a green fluorescent protein (GFP)-expressing oncolytic herpes virus to enable real-time intraoperative detection of breast cancer lymph node metastases.

Summary Background Data: Axillary lymph node status is the most important factor determining treatment, recurrence, and overall survival for women with breast cancer. The current methods of determining nodal status, however, have limitations. NV1066 is a novel oncolytic herpes viral strain that specifically infects cancer cells and expresses GFP.

Methods: Seven human breast cancer cell lines were infected in vitro with NV1066 and assessed for GFP expression, viral replication, and cytotoxicity. An in vivo model of breast cancer lymphatic metastasis was established in mice. Tumor-bearing mice were treated with NV1066 via injection into the primary tumor. Axillary lymph nodes were analyzed using an in vivo fluorescent imaging system. Histologic and molecular assessment of lymph nodes were performed using immunohistochemistry and reverse transcriptase PCR and operating characteristics were determined.

Results: NV1066 infected, expressed GFP, replicated within, and killed all human breast cancer cell lines in vitro. Injection of NV1066 into primary breast tumors resulted in viral transit to axillary lymph nodes, infection of lymphatic metastases, and GFP expression that was visualized with in vivo fluorescent imaging. Histologic and molecular confirmation demonstrated favorable operating characteristics of this method (sensitivity 80%; specificity 96%).

Conclusions: We introduce a novel, sensitive, and specific method of lymphatic mapping that utilizes NV1066-guided cancer cell-specific viral production of GFP to enable real-time intraoperative detection of lymphatic metastases.

(*Ann Surg* 2006;243: 824–832)

Breast cancer is the leading cause of cancer and the second leading cause of cancer-related deaths for women in the United States.[1] Axillary lymph node status is the most important factor determining treatment, recurrence, and overall survival for women with breast cancer. Complete lymphadenectomy has recently been replaced by sentinel lymph node biopsy (SLNB) for the determination of axillary lymph node status. SLNB identifies the individual lymph nodes draining the primary tumor and confers a less morbid method for determining nodal status.[2] While the benefits of SLNB have been confirmed, limitations remain, including the frequent failure to identify nodal metastases intraoperatively and a significant rate of nonsentinel node metastases despite negative sentinel lymph nodes.[3,4]

Oncolytic herpes viruses are replication-competent herpes simplex type-1 viruses (HSV) that selectively infect, replicate within, and lyse cancer cells. The therapeutic efficacy of these agents against a wide variety of experimental models of human malignancies has been demonstrated.[5–14] NV1066 is a novel oncolytic HSV strain that expresses enhanced green fluorescent protein (GFP). Infected cancer cells emit an intense green fluorescence that can be detected using novel in vivo fluorescent imaging modalities.

The current study investigates the potential of NV1066 to infect cancer cells in axillary lymph nodes following local administration into primary breast tumors and to enable the real-time intraoperative identification of lymph node metastases using in vivo fluorescent imaging to detect GFP expression.

METHODS

Cells

The human breast cancer cell lines LN435, MCF-7, T-47D, SK-BR-3, HCC38, HCC1954, and MDA-MB-435S were studied. LN435 was a kind gift of Dr. Jeffrey W. Smith

From the Departments of *Surgery and †Pathology, Memorial Sloan–Kettering Cancer Center, New York, NY.

Supported in part by Grant No. BC024118 from the U.S. Army (to Y.F.), training Grant No. T 32 CA09501 (to D.P.E and K.J.H.), AACR-AstraZeneca Cancer Research and Prevention fellowship (P.S.A), Grant Nos. RO1 CA 76416 and RO1 CA/DK80982 (to Y.F.) from the National Institutes of Health, Grant No. IMG0402501 from the Susan G. Komen Foundation (to Y.F.), and Grant No. 032047 from Flight Attendant Medical Research Institute (to Y.F.)

Reprints: Yuman Fong, MD, Gastric and Mixed Tumor Service, Department of Surgery, Memorial Sloan-Kettering Cancer Center, 1275 York Avenue, New York, NY 10021. E-mail: fongy@mskcc.org.

ISSN: 0003-4932/06/24306-0824
DOI: 10.1097/01.sla.0000219738.56896.c0

(Burnham Institute, La Jolla, CA) and was derived from lymph node metastases in mice with parental MDA-MB-435S mammary fat pad tumors.[15] LN435 cells were grown in minimum essential medium supplemented with nonessential amino acids, 1 mmol/L sodium pyruvate, 100 U/mL penicillin, 100 mg/mL streptomycin, and 10% fetal calf serum. MCF-7, T-47D, SK-BR-3, HCC38, HCC1954, MDA-MB-435S, and Vero cells were obtained from the American Type Culture Collection (Rockville, MD) and grown in the recommended media. Cells were maintained in a 5% CO_2 humidified incubator at 37°C.

Virus

NV1066 is a replication-competent, attenuated herpes simplex type-1 viral strain that expresses GFP upon infection of cancer cells. The construction of NV1066 has been described previously.[16] Derived from the F-strain of wild-type HSV-1, NV1066 is deficient for the UL23 sequence and the internal repeat sequences containing single copies of the viral genes ICP-4, ICP-0, and gamma-1 34.5. These genomic deletions decrease viral virulence and enhance tumor specificity. The transgene for enhanced GFP is inserted into the deleted internal repeat sequence region under the control of a cytomegalovirus promoter. Virus was propagated on Vero cells and titered by standard plaque assay.[13]

Fluorescent Microscopy

NV1066 infection and GFP expression in cancer cells were assessed in vitro by fluorescent microscopy. Cancer cells (5×10^4) were plated in 4-well chamber slides (Laboratory-Tek, San Diego, CA). After overnight incubation at 37°C, cells were infected with NV1066 at multiplicities of infection (MOI, ratio of viral plaque-forming units [PFU] to tumor cells) of 0.01, 0.1, or 1.0. Cells treated with phosphate-buffered saline (PBS) served as controls. Twelve hours after infection, cells were stained with 1 μg/mL of the double-stranded DNA-specific fluorochrome Hoechst 33342 (NPE Systems, Inc., Pembroke Pines, FL) and incubated for 15 minutes. Slides were examined using a Zeiss Axiovert 200M inverted stand microscope (Carl Zeiss, Inc., Oberkochen, Germany) and the MetaMorph Imaging System (Universal Imaging Corporation, Downingtown, PA). Cells were examined under bright-field and using a DAPI fluorescent filter to assess cellular and nuclear morphology and viability. To confirm specificity of infection, cancer cells were coincubated with lymphocytes isolated from normal murine lymph nodes, infected with NV1066, and imaged as above.

Viral Replication Assay

Standard plaque assays quantified viral replication following infection with NV1066. LN435 cells (3×10^4) were plated in 12-well flat-bottom assay plates in 2 mL of media. After overnight incubation, cells were treated with NV1066 at an MOI of 0.1. Vehicle treated cells served as controls. Supernatants and cells were collected for 7 days. Three freeze-thaw lysis cycles released intracellular viral particles. Serial dilutions of supernatants and cell lysates were cultured on confluent layers of Vero cells and titers were determined 72 hours later.

Cytotoxicity Assay

Dose-dependent assays were used to assess cytotoxicity of NV1066 against breast cancer cell lines. LN435 cells (3×10^4) were grown in 12-well flat-bottom plates in 1 mL of media. After overnight incubation, cells were treated with NV1066 at MOIs of 0.01, 0.1, and 1.0. Vehicle treated cells served as controls. Media was removed daily and cells were lysed with 1.35% Triton-X solution to release intracellular lactate dehydrogenase. Standard lactate dehydrogenase assay was performed using the Cytotox 96 nonradioactive cytotoxicity assay (Promega, Madison, WI) and a microplate reader (EL321e, Bio-Tek Instruments, Winooski, VT). Results are expressed as the percentage of surviving control cells.

Development of a Breast Cancer Lymphatic Metastasis Animal Model

Animal experiments were performed with the approval of the Memorial Sloan-Kettering Institutional Animal Care and Use Committee. Six to 8-week-old female athymic mice (National Cancer Institute, Bethesda, MD) were housed in temperature- and light-controlled rooms. Food and water were provided ad libitum. Mice were anesthetized with inhalational isoflurane for all procedures and killed by CO_2 inhalation.

LN435 was previously shown to consistently metastasize to lymph nodes.[15] Primary breast tumors were established by implanting 1 mm^3 biopsies of existing LN435 primary mammary fat pad mammary fat pad tumors into the third thoracic mammary fat pad.

To confirm the normal lymphatic drainage pattern of the primary tumor site, 1% isosulfan blue dye (50 μL) was injected into the third mammary fat pad of mice (n = 3). Two minutes after injection, animals were killed and all lymph node basins were surgically exposed. Draining nodes were identified by the uptake of blue dye.

Lymph Node Imaging

Ten weeks after tumor implantation, 10 animals were treated with intratumoral injections of 5×10^6 PFU of NV1066 in 50 μL PBS on treatment days 0 and 5. Forty-eight hours after treatment, mice were killed and the lymph node basins were surgically exposed. Lymph nodes were imaged using the Leica MZFL3 Stereomicroscope (Leica Microsystems, Germany) in both bright-field and fluorescent modes. The Retiga EX digital CCD camera (Qimaging, Burnaby, Canada) was used for image capture. Animals harboring tumor treated with 2 intratumoral injections of PBS (n = 3) and animals without tumor treated with NV1066 (regimen as above) (n = 3) served as controls.

Histologic and Molecular Analysis of Lymph Nodes

Immediately after imaging, lymph nodes were harvested, fixed in 10% buffered formalin acetate, and embedded in paraffin; 8-μmol/L sections were stained with hematoxylin and eosin and examined for tumor deposits. Serial sections were assessed for GFP expression via fluorescent microscopy (Axiovert 200 microscope, Carl Zeiss, Inc.) to confirm the localization of GFP expression to metastatic foci. Immunohistochemistry was performed using a polyclonal antibody to

TABLE 1. RT-PCR Primer Sequences

Gene	Forward Sequence (5′−3′)	Reverse Sequence (5′−3′)
Alpha-6 Integrin	CATCTCCTCCCTGAGCACATATT	GGGCTCCAATAACTATATCTTGC
ICP-0	ATGTTTCCCGTCTGGTCCAC	5′-CCCTGTCGCCTTACGTGAA
18S	GTAACCCGTTGAACCCCATT	CCATCCAATCGGTAGTAGCG

tumor marker S-100 (Dako, Carpinteria, CA). All results were confirmed by a blinded pathologist (S.C.).

Ten weeks after tumor implantation, 10 animals were treated and used for molecular confirmation of tumor and viral presence. Forty-eight hours after viral administration, axillary lymph nodes were imaged for GFP expression and then harvested, bisected, and snap frozen in liquid nitrogen for RNA and DNA isolation. Total RNA was isolated from tissue per a standard protocol using the TRIZOL reagent (Invitrogen Corp., Carlsbad, CA). Genomic DNA was isolated using a standard protocol (DNeasy Tissue Kit, Qiagen Inc., Valencia, CA). SYBR green-based real-time quantitative polymerase chain reaction (PCR) was performed using an ABI Prism 7900HT Sequence Detection System (Applied Biosystems, Foster City, CA). Tumor presence was determined using the tumor epithelial marker alpha-6 integrin, viral presence was confirmed using the HSV-1 ICP-0 immediate early gene and coamplification of the 18S housekeeping gene was used for normalization (Table 1).

RESULTS

NV1066 Infects and Expresses GFP in LN435 Cells

LN435 human breast cancer cells express GFP following viral infection. Representative images are shown in Figure 1. LN435 cells treated with NV1066 strongly expressed GFP 12 hours following infection at all MOIs tested (Fig. 1A). Conversely, viable LN435 cells incubated with vehicle alone (Fig. 1B) and normal lymphocytes coincubated with cancer cells infected with NV1066 (Fig. 1C) did not express GFP.

NV1066 Replicates Within and Is Cytotoxic to LN435 Cells

LN435 cells support viral replication. Five days following infection at an MOI of 0.1, viral titers peaked at 2.9×10^6 PFU representing a 970-fold amplification in viral titer compared with the initial infective dose (3000 PFU) (Fig. 2A). Additionally, NV1066 demonstrates dose-dependent cytotoxicity over a 100-fold range of viral doses (Fig. 2B). Three days after infection at an MOI of 1.0, 94% (±1%) of cells were killed. By day 7, nearly 100% of cells were killed. Seven days following infection at a 10-fold lower MOI (0.1), 95% (±1%) of cells were killed. Even at an MOI of 0.01, representing 1 viral particle per 100 cancer cells, 85% (±4%) of cells are killed 7 days after infection. The dramatic increase in cell kill observed 3 to 4 days after infection at an MOI of 0.1 coincides with the steep rise in viral titer and indicates that successful viral progeny production during the early infection ultimately results in near complete cell kill after 7 days.

NV1066 Infects, Expresses GFP Within, and Lyses a Range of Breast Cancer Cell Lines

Estrogen receptor (ER)-positive and progesterone receptor (PR)-positive cell lines (MCF-7, T-47D), ER-negative and PR-negative cell lines (SK-BR-3, HCC38, HCC1954,

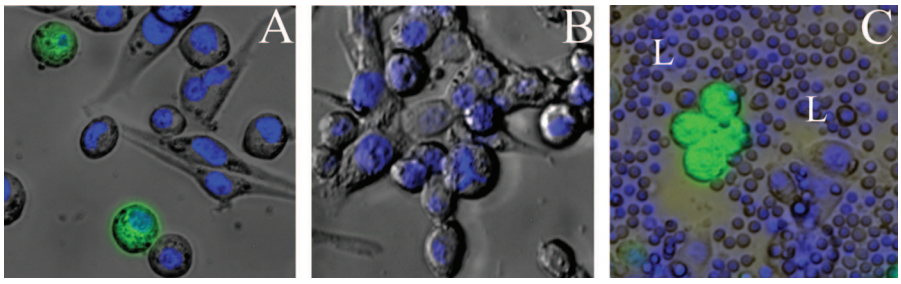

FIGURE 1. NV1066 infects and expresses GFP in LN435 breast cancer cells. Monolayer cultures of LN435 cells were infected with NV1066 at MOIs of 0.01, 0.1, or 1.0 in 100 μL PBS or vehicle alone. Additional cells were coincubated with lymphocytes isolated from normal murine lymph nodes. Twelve hours following infection, cells were stained with Hoechst and subsequently examined by bright-field and fluorescent microscopy. DAPI (Hoechst) fluorescent detection was used to assess nuclear morphology and cellular viability, and GFP fluorescent detection was used to assess NV1066 infection and cellular expression of GFP. Representative overlay images constructed by digital superimposition of corresponding bright-field, DAPI, and GFP frames are shown. LN435 cells treated with NV1066 strongly expressed GFP 12 hours following infection at all MOIs tested (A, MOI 0.1, original magnification ×40). Control LN435 cells incubated with vehicle alone (B, MOI 0.1, original magnification ×40) and murine lymphocytes (L) coincubated with cancer cells (C, MOI 0.1, original magnification ×20) did not express GFP demonstrating the specificity of viral infection and GFP expression for cancer cells. MOI (multiplicity of infection) represents the ratio of the number of viral particles to the number of tumor cells. DAPI, 4′,6-diamidino-2-phenylindole (double-stranded DNA staining); GFP, green fluorescent protein.

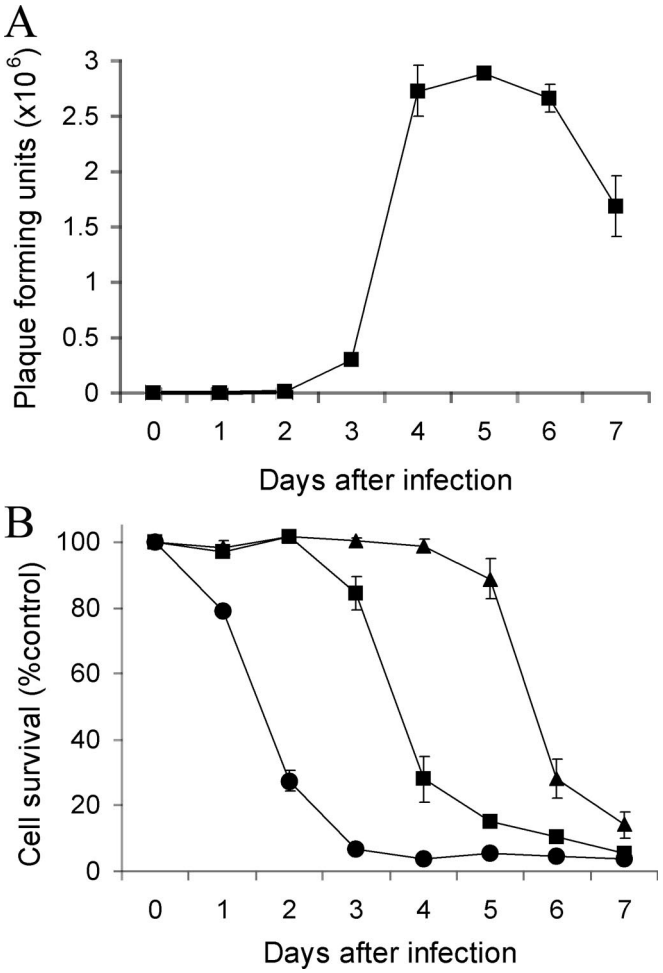

FIGURE 2. NV1066 replicates within and is cytotoxic to LN435 breast cancer cells. A, Monolayer cultures of LN435 cells were treated with NV1066 at an MOI of 0.1 (3000 PFU). Viral progeny were quantified daily after infection for 7 days by standard plaque assay. Mean PFU for triplicate samples are plotted (±standard error of the mean). B, Monolayer cultures of LN435 cells were infected with NV1066 at MOIs of 0.01 (triangle), 0.1 (square), and 1.0 (circle). Cytotoxicity assays were used to measure cell kill daily after infection for 7 days. Mean cellular survival for triplicate samples is plotted as a percentage of control uninfected cells (±standard error of the mean). MOI (multiplicity of infection) represents the ratio of the number of viral particles to the number of tumor cells. PFU, plaque-forming units.

MDA-MB-435S), low HER-2/neu expressing cell lines (MCF-7, HCC38, MDA-MB-435S), an intermediate HER-2/neu expressing cell line (T-47D), and high HER-2/neu expressing cell lines (SK-BR-3, HCC1954) all were infected, expressed GFP, and lysed by NV1066 at all MOIs tested. Cell kill 7 days after infection at an MOI of 1.0 for these cell lines ranged from 87% to 99%.

NV1066-Guided GFP-Mediated Fluorescent Detection of Lymph Node Metastases

We have established a reliable murine model of breast cancer axillary lymph node metastases that yields nodal metastases in 40% of animals. Lymphatic mapping after injection of 1% isosulfan blue dye into the third mammary fat pad demonstrated intense uptake of blue dye in ipsilateral axillary nodes (data not shown). Contralateral axillary and ipsilateral cervical, inguinal, retroperitoneal, and mediastinal lymph nodes did not stain blue.

We demonstrated that GFP expression in NV1066-infected axillary lymph node metastases can be detected with in vivo fluorescent imaging. Representative images are shown in Figure 3. Mice with nodal metastases frequently demonstrated enlarged ipsilateral axillary lymph nodes (Fig. 3A). Involved lymph nodes exhibited intense focal expression of GFP when imaged via fluorescent stereomicroscopy (Fig. 3C, D). Lymph nodes not harboring tumor and control lymph nodes did not express GFP.

Histologic and Molecular Analysis of Lymph Nodes

Histologic examination confirmed the presence of tumor and GFP in positive lymph nodes (Fig. 4). Furthermore, areas of GFP expression localized to tumor foci in lymph nodes. Absence of tumor and GFP in lymph negative lymph nodes (as determined by fluorescent imaging) was similarly confirmed by microscopic analysis.

RT-PCR detection of the tumor-specific epithelial marker alpha-6 integrin in lymph nodes demonstrated favorable operating characteristics of NV1066-mediated GFP-guided detection of breast cancer lymph node metastasis (Table 2). Thirty lymph nodes (average, 3 per animal) were analyzed. Five of 30 lymph nodes (17%) analyzed were determined to harbor tumor by RT-PCR amplification of alpha-6 integrin. Four of 5 (80%) of these positive lymph nodes expressed GFP when examined with fluorescent imaging. One of 25 (4%) lymph nodes not determined to harbor tumor cells by RT-PCR was reported to express GFP via fluorescent imaging. As such, the operating characteristics are as follows: sensitivity = 80%, specificity = 96%, positive predictive value = 80%, and negative predictive value = 96%.

PCR amplification of the viral gene ICP-0 detected viral DNA in 3 of 5 (60%) lymph nodes that were GFP positive. Viral DNA was not detected in any of the 25 lymph nodes that were GFP negative. The apparent absence of virus in 2 positive lymph nodes is likely due to sampling error, as these lymph nodes contained focal disease yet were bisected for analysis.

DISCUSSION

Lymph node status is a powerful prognostic factor for many cancers. For women with breast cancer, axillary lymph node status is the most important factor determining treatment, recurrence, and overall survival. Until recently, complete lymphadenectomy was routinely performed to stage patients with breast cancer. This practice, however, subjected many women with early stage disease to a morbid procedure with no benefit. It further hindered the identification of micrometastases due to the impracticality of performing extensive histologic analyses on a large number of resected nodes.

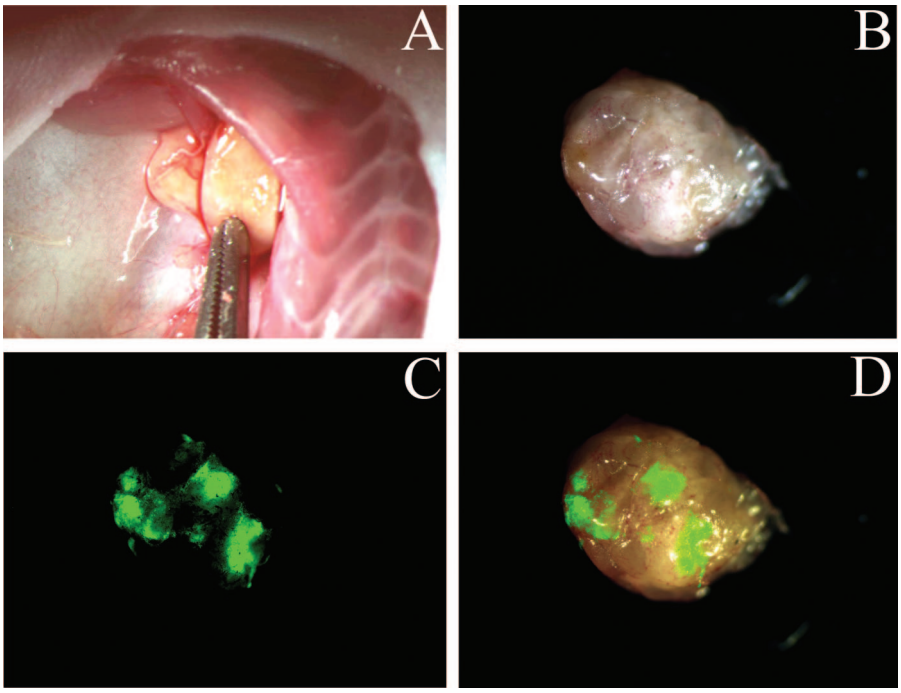

FIGURE 3. NV1066-guided GFP-mediated fluorescent detection of lymph node metastases. LN435 human breast cancer xenograft biopsies were microsurgically implanted into the third right mammary fat pad in female athymic mice. After 10 weeks, 5×10^6 PFU of NV1066 was injected into the primary tumor on treatment days 0 and 5. Forty-eight hours later, animals were killed and axillae were explored. Representative images are shown. A, Right axilla demonstrating two enlarged axillary lymph nodes (original magnification ×5). B, Bright-field image of single enlarged axillary lymph node ex vivo (original magnification ×10). C, GFP fluorescent image of lymph node ex vivo demonstrating foci of high GFP intensity (original magnification ×10). D, Computer-generated overlay of bright-field (B) and GFP (C) digital images (original magnification ×10).

The advent of SLNB has circumvented these shortcomings allowing a more selective approach to the identification of regional lymph node metastases.[2] SLNB relies on vital dye enhancement and nodal uptake of radioactive colloid to identify the individual lymph nodes draining the primary tumor. This method is generally successful for the identification of sentinel nodes, the status of which is considered representative of the entire nodal basin. SLNB has resulted in accurate axillary staging with decreased morbidity when compared with complete lymph node dissection and has become an important method for staging women with early breast cancer.[4]

The limitations of SLNB, however, have recently become apparent. Intraoperative analyses of sentinel nodes fail to identify metastatic disease in 15% to 24% of patients.[17,18] Lymphatic metastases missed intraoperatively mandate a second operation for completion axillary lymph node dissection. In addition, 7% to 19% of patients with negative sentinel nodes are found to have metastases in nonsentinel nodes.[19–22] SLNB can be cumbersome and labor-intensive requiring multiple preoperative interventions. Injection of vital blue dye can stain the breast for many months and is associated with a 1% risk of anaphylaxis.[23–26] Administration of the radioactive colloid tracer requires well-coordinated interdepartmental planning to avoid operating room delays. Most importantly, recently presented data from a multi-institutional trial following over 5500 women indicates that morbidity following SLNB is greater than expected with rates of lymphedema, axillary paresthesias, and reduced upper extremity range of motion approaching 7%, 9%, and 4%, respectively.[26]

We introduce a novel method of lymphatic mapping that uses cancer cell-specific viral production of GFP to detect tumor cells in lymph nodes. We have shown that NV1066 travels to regional lymph nodes after administration into the primary tumor where it infects cancer cells. Infection results in expression of GFP, the protein product of which

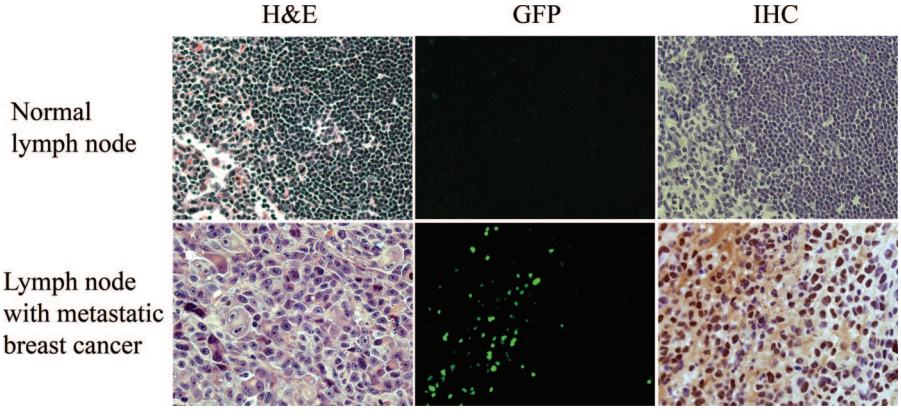

FIGURE 4. Histologic analysis of tumor and GFP in lymph nodes. Serial sections of a negative lymph node (no GFP expression by in vivo fluorescent imaging) is confirmed to have no tumor nor GFP expression when examined with hematoxylin and eosin (H&E), fluorescent microscopy, and immunohistochemistry (original magnification ×20) (top row). Histologic analysis of a positive lymph node (strong GFP expression by in vivo fluorescent imaging) is confirmed to harbor tumor and express GFP (original magnification ×20) (bottom row). GFP, green fluorescent protein.

TABLE 2. Operating Characteristics of NV1066-Guided Fluorescent Detection of Lymph Node Metastases

	GFP Positive	GFP Negative
Alpha-6 Integrin Positive	4	1
Alpha-6 Integrin Negative	1	24
Sensitivity		80%
Specificity		96%
Positive predictive value		80%
Negative predictive value		96%

Thirty lymph nodes from 10 animals were assessed for GFP expression via in vivo fluorescent imaging and tumor presence by RT-PCR amplification of the LN435 epithelial tumor marker alpha-6 integrin.

emits intense green fluorescence that can be visualized by novel in vivo fluorescent imaging modalities. The real-time intraoperative detection of lymph node metastases distinguishes this technique from SLNB. Regional lymph nodes harboring cancer cells can be identified regardless of "sentinel" or "nonsentinel" status and therefore may reduce the false-negative rate associated with SLNB. This viral technique does not just identify the most proximal lymph nodes to the index cancer, it may identify all positive lymph nodes in a drainage basin. As such, this method may ultimately preclude the unnecessary resection of negative lymph nodes and avoid its inherent morbidity. This proof-of-concept study also demonstrates that herpes-guided GFP detection of lymphatic metastases can be a highly sensitive and specific technique comparing favorably with standard methods.

Furthermore, while SLNB is purely diagnostic, the use of oncolytic herpes viruses may confer an additional therapeutic advantage. Extensive work in our laboratory and others has demonstrated that parental oncolytic HSV strains are highly effective in the treatment of a wide variety of experimental models of cancer including lung, colorectal, prostate, pancreatic, hepatobiliary, gastric, esophageal, and breast.[5–14] More recently, Stiles et al[27] showed that intratumoral injection of NV1066 significantly suppressed tumor growth in a murine flank tumor model of esophageal carcinoma. Stanziale et al[16] subsequently demonstrated that administration of NV1066 into the peritoneal cavity of mice harboring gastric carcinomatosis resulted in a dose-dependent reduction in tumor burden. The therapeutic efficacy of NV1066 in the treatment of locoregional breast cancer in our model is currently being assessed.

These studies were also first to demonstrate that NV1066-mediated GFP expression localizes to tumor deposits, spares normal tissues, and identifies intraperitoneal metastases in vivo using a novel laparoscopic imaging system with GFP-detection capabilities (Olympus America, Inc., Melville, NY).[16,27] This laparoscopic system enables real-time intraoperative visualization in both bright-field and fluorescent modes and readily identifies intraperitoneal metastases less than 2 mm in diameter. A similar in vivo fluorescent imaging system could be employed in breast cancer to permit fluorescence-directed detection of axillary lymph node metastases.

SLNB has also become the standard of care for regional staging of melanoma, and is being investigated for use in gastrointestinal, thoracic, thyroid, genitourinary, and head and neck malignancies.[28–30] To date, we have shown that NV1066 infects and expresses GFP in over 110 cancer cell lines from over 16 different tissues of origin. We have learned from these studies that GFP can be detected as early as 2 to 6 hours following viral infection. NV1066 carries "enhanced" GFP, which produces a 6-fold stronger fluorescent signal and matures 4-fold faster than conventional GFP, reducing the lag time between synthesis and detection. Furthermore, amplification of the administered viral dose enables treatment with low viral titers. In vitro flow cytometric studies have demonstrated that even at an MOI of 0.01, representing 1 viral particle per 100 cancer cells, approximately 100% of cultured cancer cells express GFP 5 to 7 days following infection. Lastly, this study confirms that expression of GFP in nonsurface metastases can be visualized. The depth and limits of detection are presently being assessed by us.

The potential toxicity of these agents has also been extensively investigated. Oncolytic herpes viruses are highly specific for infection of cancer cells sparing normal cells. Numerous investigations using NV1066 and parental oncolytic HSV strains have shown no observable toxicity in rodent models. Animals maintained their weights and demonstrated no alteration of food and water intake, grooming, or any other behavioral alterations during the treatment period. Furthermore, immunohistochemical and PCR analyses consistently demonstrate the complete absence of viral particles in noncancerous tissues. The safety of these viruses has been tested in preclinical toxicology studies in *Aotus* monkeys that are exquisitely sensitive to wild-type herpes viral infections.[31,32] These monkeys demonstrated little toxicity when administered attenuated virus at potentially therapeutic doses. Additionally, the favorable safety profile of parental oncolytic HSV strains has been established in phase I human clinical trials.[33]

Herpes-guided lymphatic mapping is a novel, sensitive, and specific technique that uses cancer cell-specific viral production of GFP to enable detection of lymph node metastases. Advantages of this method compared with standard techniques include real-time intraoperative detection of sentinel and nonsentinel lymphatic metastases and the potential for a concomitant therapeutic effect. This technique may benefit the multitude of patients with any one of the many cancers that exhibit predictable patterns of regional lymph node metastases.

ACKNOWLEDGMENTS

The authors thank Irina Linkov, Dr. Katia Manova, Rumana Huq, and Tao Tong for their technical assistance, and offer very special thanks to Liza Marsh for her editorial assistance.

REFERENCES

1. Jemal A, Murray T, Ward E, et al. Cancer statistics, 2005. *CA: Cancer J Clin.* 2005;55:10–30.
2. Morton DL, Wen DR, Wong JH, et al. Technical details of intraoperative lymphatic mapping for early stage melanoma. *Arch Surg.* 1992;127: 392–399.
3. Veronesi U, Galimberti V, Mariani L, et al. Sentinel node biopsy in breast cancer: early results in 953 patients with negative sentinel node biopsy and no axillary dissection. *Eur J Cancer.* 2005;41:231–237.

4. Kelley MC, Hansen N, McMasters KM. Lymphatic mapping and sentinel lymphadenectomy for breast cancer. *Am J Surg*. 2004;188:49–61.
5. Andreansky S, Soroceanu L, Flotte ER, et al. Evaluation of genetically engineered herpes simplex viruses as oncolytic agents for human malignant brain tumors. *Cancer Res*. 1997;57:1502–1509.
6. Chambers R, Gillespie GY, Soroceanu L, et al. Comparison of genetically engineered herpes simplex viruses for the treatment of brain tumors in a scid mouse model of human malignant glioma. *Proc Natl Acad Sci USA*. 1995;92:1411–1415.
7. Chahlavi A, Todo T, Martuza RL, et al. Replication-competent herpes simplex virus vector G207 and cisplatin combination therapy for head and neck squamous cell carcinoma. *Neoplasia*. 1999;1:162–169.
8. Advani SJ, Chung SM, Yan SY, et al. Replication-competent, nonneuroinvasive genetically engineered herpes virus is highly effective in the treatment of therapy-resistant experimental human tumors. *Cancer Res*. 1999;59:2055–2058.
9. Mineta T, Rabkin SD, Yazaki T, et al. Attenuated multi-mutated herpes simplex virus-1 for the treatment of malignant gliomas. *Nat Med*. 1995;1:938–943.
10. Wong RJ, Kim SH, Joe JK, et al. Effective treatment of head and neck squamous cell carcinoma by an oncolytic herpes simplex virus. *J Am Coll Surgeons*. 2001;193:12–21.
11. McAuliffe PF, Jarnagin WR, Johnson P, et al. Effective treatment of pancreatic tumors with two multimutated herpes simplex oncolytic viruses. *J Gastrointest Surg*. 2000;4:580–588.
12. Bennett JJ, Kooby DA, Delman K, et al. Antitumor efficacy of regional oncolytic viral therapy for peritoneally disseminated cancer. *J Mol Med*. 2000;78:166–174.
13. Kooby DA, Carew JF, Halterman MW, et al. Oncolytic viral therapy for human colorectal cancer and liver metastases using a multi-mutated herpes simplex virus type-1 (G207). *FASEB J*. 1999;13:1325–1334.
14. Yazaki T, Manz HJ, Rabkin SD, et al. Treatment of human malignant meningiomas by G207, a replication-competent multimutated herpes simplex virus 1. *Cancer Res*. 1995;55:4752–4756.
15. Lee H, Lin EC, Liu L, et al. Gene expression profiling of tumor xenografts: in vivo analysis of organ-specific metastasis. *Intl J Cancer*. 2003;107:528–534.
16. Stanziale SF, Stiles BM, Bhargava A, et al. Oncolytic herpes simplex virus-1 mutant expressing green fluorescent protein can detect and treat peritoneal cancer. *Hum Gene Ther*. 2004;15:609–618.
17. Veronesi U, Paganelli G, Galimberti V, et al. Sentinel-node biopsy to avoid axillary dissection in breast cancer with clinically negative lymph-nodes. *Lancet*. 1997;349:1864–1867.
18. Viale G, Bosari S, Mazzarol G, et al. Intraoperative examination of axillary sentinel lymph nodes in breast carcinoma patients. *Cancer*. 1999;85:2433–2438.
19. Veronesi U, Paganelli G, Viale G, et al. Sentinel lymph node biopsy and axillary dissection in breast cancer: results in a large series. *J Natl Cancer Inst*. 1999;91:368–373.
20. Harlow SP, Krag DN, Julian TB, et al. Prerandomization Surgical Training for the National Surgical Adjuvant Breast and Bowel Project (NSABP) B-32 trial: a randomized phase III clinical trial to compare sentinel node resection to conventional axillary dissection in clinically node-negative breast cancer. *Ann Surg*. 2005;241:48–54.
21. Feldman SM, Krag DN, McNally RK, et al. Limitation in gamma probe localization of the sentinel node in breast cancer patients with large excisional biopsy. *J Am Coll Surgeons*. 1999;188:248–254.
22. McMasters KM, Tuttle TM, Carlson DJ, et al. Sentinel lymph node biopsy for breast cancer: a suitable alternative to routine axillary dissection in multi-institutional practice when optimal technique is used. *J Clin Oncol*. 2000;18:2560–2566.
23. Montgomery LL, Thorne AC, Van Zee KJ, et al. Isosulfan blue dye reactions during sentinel lymph node mapping for breast cancer. *Anesth Analg*. 2002;95:385–388.
24. Leong SP, Donegan E, Heffernon W, et al. Adverse reactions to isosulfan blue during selective sentinel lymph node dissection in melanoma. *Ann Surg Oncol*. 2000;7:361–366.
25. Cimmino VM, Brown AC, Szocik JF, et al. Allergic reactions to isosulfan blue during sentinel node biopsy: a common event. *Surgery*. 2001;130:439–442.
26. Wilke LG, McCall LM, Whitworth PW, et al. Surgical Complications associated with sentinel node lymph node biopsy: results from a Prospective International Cooperative Group Trial. *Proceedings of the 58th Annual Cancer Symposium of the Society of Surgical Oncology*. 2005; 12(suppl):27.
27. Stiles BM, Bhargava A, Adusumilli PS, et al. The replication-competent oncolytic herpes simplex mutant virus NV1066 is effective in the treatment of esophageal cancer. *Surgery*. 2003;134:357–364.
28. Soltesz EG, Kim S, Laurence RG, et al. Intraoperative sentinel lymph node mapping of the lung using near-infrared fluorescent quantum dots. *Ann Thorac Surg*. 2005;79:269–277.
29. Kitagawa Y, Fujii H, Kumai K, et al. Recent advances in sentinel node navigation for gastric cancer: a paradigm shift of surgical management. *J Surg Oncol*. 2005;90:147–152.
30. Gipponi M, Solari N, Di Somma FC, et al. New fields of application of the sentinel lymph node biopsy in the pathologic staging of solid neoplasms: review of literature and surgical perspectives. *J Surg Oncol*. 2004;85:171–179.
31. Todo T, Feigenbaum F, Rabkin SD, et al. Viral shedding and biodistribution of G207, a multimutated, conditionally replicating herpes simplex virus type 1, after intracerebral inoculation in aotus. *Mol Ther*. 2000;2: 588–595.
32. Varghese S, Newsome JT, Rabkin SD, et al. Preclinical safety evaluation of G207, a replication-competent herpes simplex virus type 1, inoculated intraprostatically in mice and nonhuman primates. *Hum Gene Ther*. 2001;12:999–1010.
33. Fong Y, Kemeny N, Jarnagin W, et al. Phase 1 study of a replication-competent herpes simplex oncolytic virus for treatment of hepatic colorectal metastases. *Proc Am Soc Clin Oncol*. 2002;21:8a.

Discussions

DR. KIRBY L. BLAND (BIRMINGHAM, ALABAMA): As you have heard in the presentation, this technique has the potential to benefit various organ site cancers that exhibit predictable patterns of regional lymphatic metastases. The authors have studied use of green fluorescent protein (GFP) expressing oncolytic herpes virus to enable real-time intraoperative detection of these metastases in a breast cancer murine model. This has particular relevance in breast cancer as axillary lymphatic metastases currently represent the most useful prognostic variable in the most common female carcinoma. The lymph node metastasis status remains a very powerful predictive factor, and the use of sentinel lymph node biopsy developed in human melanoma patients (Don Morton and associates) is now being transferred to various organ system cancers, including breast, gastric, colon, and esophageal neoplasms. The most common indication in its application has been for breast and melanoma. Using this methodology of sentinel node biopsy has allowed an accurate staging that decreases morbidity when compared with conventional lymph node dissection. As indicated by the authors in their manuscript, intraoperative analyses of the sentinel lymph node fails to pathologically identify metastatic disease in 15% to 24% of patients; in addition, as great as one fifth of all patients with negative sentinel nodes are found to have metastasis in non-sentinel bearing lymphatics.

The authors have therefore introduced a novel method utilizing cancer cell-specific viral production of GFP to detect tumor cells in lymphatics. Regional lymph nodes that harbor

these cancer cells can be identified, regardless of their sentinel or non-sentinel status, and therefore may reduce the false-negative rate associated with the sentinel node biopsy. As you have heard in the presentation, herpes-guided GFP detection of lymphatic metastases can be a highly sensitive and specific technique that compares favorably with standard measures.

The authors have suggested and confirmed in their laboratory that the novel oncolytic herpes viral strain (NV1066) specifically infects cancer cells and expresses GFP allowing intraoperative detection of these metastases. Indeed, histologic and molecular confirmation demonstrated favorable operating characteristics of this method with a sensitivity of 80% and a specificity of 96%. This converts to a positive predictive value of 80% and a negative predictive value of 96%. My question therefore is: what do you anticipate and have you now had experience with human?

What is the evidence and your experience in human tumor cell lines that there will be expression of GFP oncolytic herpes virus in vivo to allow intraoperative detection of breast cancer lymphatic metastasis in humans?

It would appear that in the seven human cell lines that have been infected in vitro with NV1066 and assessed for GFP expression, your data suggest viral transit to lymphatics and infection of the metastases. With this high sensitivity and specificity in the animal model, have you obtained an IND number for injection of GFP from your Institutional Review Board to study such technique?

Dr. Karen J. Hendershott (New York, New York): The question of moving this from an animal model study into a human setting is obviously very important. This study I just presented is a proof of principal study that is meant to just establish the concept that we could localize lymph nodes using this technology.

The NV1066 virus is a second-generation herpes virus, and most of our experience using human trials comes from the parent viruses. We had attained an IND for studying the virus, NV1020, and have completed a phase 1 trial at our institution using this virus to treat liver cancer. We are looking at moving on to a phase 2 trial as well. So we are working in that direction.

Everything that we look at in terms of in vitro data and also with our work with animal models suggests that the NV1066 virus behaves similarly to the parental virus. So I can at least hypothesize that it should move well into clinical trials. In terms of in vivo detection in humans, it certainly has the potential to go forward and do that.

In our laboratory, we actually have a modified Olympus laparoscope that we have used in animal models, and Steve Stanziale in our lab was able to detect intraperitoneal metastases as small as 2 mm using this laparoscope in a mouse model. So I think that is one of the areas where we have the greatest opportunity, using the laparoscopic system to expand this technology into humans.

Dr. Michael J. Edwards (Little Rock, Arkansas): You showed that these viral vectors will track through the lymphatics in an effective way to arrive at the tumor cell. Could you comment about the ability of these agents to track to other common sites of metastases (ie, the brain, the liver, the bone)? Are they as likely to be effective at that level as they are in the lymph nodes?

I was a little surprised that you were able to grossly detect the fluorescence in the axilla. What is the size of the lymph node in this model? How does that compare to the size of the lymph node in a human? The reason I bring that up is one of the great things about sentinel lymph node staging, as the current state of the art, is the ability to detect tiny deposits of disease that are still clinically relevant at the 2 mm or so size.

Should a 2-mm metastasis, for example, fluoresce through a lymph node? Your sensitivity was 80%; what do you surmise was the reason for not detecting the one nodal metastasis? Is it related to the size of the metastasis?

Finally, in the early days of sentinel lymph node staging, we had advocates of the blue dye and advocates of technetium sulfur colloid. What we learned at the end of the day, and Dr. McMasters of this organization has so eloquently presented, that when we combined the two it worked much, much better, and the combination became the state of the art.

You have suggested that this new technique could potentially replace the current state of the art and pointed out many "Achilles tendons" of the current state-of-the-art sentinel lymph node staging. I remind you, however, that the Louisville database has thousands of lymph nodes that have been analyzed defining sentinel lymph node staging. We are talking about five lymph nodes today. How do you see this unfolding for the future? What is the next step?

Dr. Karen J. Hendershott (New York, New York): In terms of the question where you asked about utility for other sites of metastases, this is really intriguing because of an unexpected finding in our study. As we serially passaged the tumors, the animals went on to develop not only axillary lymph node metastases but also metastatic disease in the lungs and even occasionally intra-abdominal disease.

What we found was that after we administered the virus into the tumor, namely, at the site in the mammary fat pad, the green fluorescence was expressed not only within those lymph node metastases but also within the lung metastases. We also detected mediastinal nodes that were also positive that fluoresced green and also intra-abdominal deposits, which suggests that there is hematogenous as well as lymphatic distribution of the virus. And this is consistent with what we have seen in other animal models where we have looked at peritoneal metastases and thoracic metastases. So I think it does

have potential to be used to detect distant disease, and that is one of the areas that we are continuing to explore.

In terms of the lymph nodes in mice, it can be variable. The average lymph node size is between 2 and 5 mm in these animals. Their axillary basin usually contains two to three lymph nodes. We confirmed through a blue dye study that the drainage pattern is similar to what we have seen in humans prior to initiating our current study.

In terms of your question about depth of penetration of the fluorescence, I don't have exact data to answer that question. But anecdotally, I can tell you that where we had a small tumor deposit in an animal behind the pectoralis muscle, we were actually able to see that green fluorescence all the way through the pectoralis muscle. Now, in a mouse that is probably 2 mm. But that still suggests that we are getting fairly good penetration of the fluorescence.

I don't have a good answer for how we missed that one lymph node. As I mentioned, we used RT-PCR as our gold standard, which is holding us perhaps to a higher standard than most folks would. So we might have simply picked up very small amounts of disease that might not even have been clinically relevant.

But one of the limitations of the study is the small number of positive nodes. We have a sensitivity of 80% from missing one lymph node. I suspect those numbers would look better if we were able to increase the number of positive lymph nodes. And that was simply a challenge of the animal model.

Dr. David J. Cole (Charleston, South Carolina): A couple of questions: The intriguing part of this is the potential clinical application. And I think the mark that you would want to have is 100% sensitivity to the final pathology, not the 59% that you presented. So although maybe the 80% of your test is better, it is not good enough to make clinical decisions on. I would be concerned that an ability to detect 2 mm of cancer cells in a lymph node will still leave you short of the mark. So I would be curious what your thoughts are in terms of value sensitivity when compared to final pathology.

Also, you really didn't mention a significant amount of work already done. There are molecular markers already well defined with a high level of sensitivity for the detection of micrometastatic disease in lymph nodes. So I would think you would ultimately need to compare to other molecular technologies that are currently out there in terms of how this new technology would come up to that mark.

Dr. Karen J. Hendershott (New York, New York): First of all, I agree with your concerns. And I think there are a couple of important points to make of how this technology differs from sentinel lymph node biopsy.

First of all, what we are talking about is intraoperative detection of lymph node metastases and to see if we can prevent the quarter of women who have falsely negative nodes intraoperatively from having to go back and have a second surgery.

Secondly, our technique is a little bit different. The virus doesn't just show you where the lymph tracks to, which is basically what you are looking at with a sentinel lymph node biopsy. What our virus allows to us do is to evaluate for cancer in all the lymph nodes within the basin regardless of their sentinel status or not, which I think is an advantage here. It is an advantage in breast cancer, but I think it is an even more significant advantage when you start applying this to other cancers, like gastric cancer, head and neck cancer, melanoma, and colon cancer, which is one of the next steps that we are going to be evaluating.

In addition, there is nothing that precludes the use of the radioactive dye at the same time as using the virus. I certainly would see this as an adjuvant at the initial stages of moving us into clinical management. I think that those are important factors to consider.

Finally, one advantage of the viral detection method is that it doesn't preclude the use of molecular markers. In fact, the fluorescence can be used to highlight cancer cells so a more in depth analysis can be applied to these pre-selected cells. Just like SLNB allowed us to perform focused analyses of a small number of lymph nodes, virally-directed green fluorescence can facilitate in an in depth study of cancerous cells which is an important advantage with the development of molecular-targeted therapies.